HHS Public Access

Author manuscript

Nat Mater. Author manuscript; available in PMC 2017 February 15.

Published in final edited form as:

Nat Mater. 2016 December ; 15(12): 1297–1306. doi:10.1038/nmat4725.

N-Cadherin adhesive interactions modulate matrix mechanosensing and fate commitment of mesenchymal stem cells

Brian D. Cosgrove[1,2,3], **Keeley L. Mui**[4], **Tristan P. Driscoll**[1,2,3], **Steven R. Caliari**[2], **Kush D. Mehta**[1,2], **Richard K. Assoian**[4], **Jason A. Burdick**[2], and **Robert L. Mauck**[1,2,3,†]

[1]McKay Orthopaedic Research Laboratory, Department of Orthopaedic Surgery, Perelman School of Medicine, University of Pennsylvania, Philadelphia, PA 19104

[2]Department of Bioengineering, University of Pennsylvania, Philadelphia, PA 19104

[3]Translational Musculoskeletal Research Center, Philadelphia VA Medical Center, Philadelphia, PA 19104

[4]Department of Pharmacology, Perelman School of Medicine, University of Pennsylvania, Philadelphia, PA 19104

Abstract

During mesenchymal development, the microenvironment gradually transitions from one that is rich in cell-cell interactions to one that is dominated by cell-extracellular-matrix (ECM) interactions. Because these cues cannot readily be decoupled in vitro or in vivo, how they converge to regulate mesenchymal stem cell (MSC) mechanosensing is not fully understood. Here, we show that a hyaluronic acid hydrogel system enables, across a physiological range of ECM stiffness, the independent co-presentation of the HAVDI adhesive motif from the EC1 domain of N-Cadherin and the RGD adhesive motif from fibronectin. Decoupled presentation of these cues revealed that HAVDI ligation (at constant RGD ligation) reduced the contractile state and thereby nuclear YAP/TAZ localization in MSCs, resulting in altered interpretation of ECM stiffness and subsequent changes in downstream cell proliferation and differentiation. Our findings reveal that, in an evolving developmental context, HAVDI/N-Cadherin interactions can alter stem cell perception of the stiffening extracellular microenvironment.

Keywords

N-Cadherin; YAP/TAZ; Mechanotransduction; Mechanosensing

†Corresponding Author: Robert L. Mauck, Ph.D., Associate Professor of Orthopaedic Surgery and Bioengineering, McKay Orthopaedic Research Laboratory, Department of Orthopaedic Surgery, University of Pennsylvania, 36th Street and Hamilton Walk, Philadelphia, PA 19104, Phone: (215) 898-3294, Fax: (215) 573-2133, lemauck@mail.med.upenn.edu.

Author Contributions

BDC, KLM, RKA, JAB, and RLM designed the studies. BDC, KLM, SRC, and KDM performed the experiments. BDC, KLM, TPD, RKA, SRC, JAB, and RLM analyzed and interpreted the data. BDC, JAB, and RLM drafted the manuscript, and all authors edited the final submission.

Main

It is well established that, in addition to soluble factors and extracellular matrix (ECM) ligands, the mechanical properties of the microenvironment can direct stem cell behavior[1–6]. Interpretation of mechanical inputs (including substrate stiffness) requires the generation of contractile forces in the cytoskeleton through which the cell actively interrogates its surroundings[7]. Above a certain threshold, this interaction induces mechanically-activated signaling to regulate cell spreading, traction[8], and RhoA activity[9] to modulate progenitor cell proliferation, migration, and differentiation[2]. The YAP/TAZ complex (Yes-associated protein/Transcriptional co-activator) has recently been implicated as an important factor in the transduction of mechanical signals[10, 11]. Two primary YAP/TAZ signaling branches are operative: 1) the Hippo pathway, in which cadherin-cadherin trans-interactions result in sequestration of YAP in the cytosol[12], and 2) a mechanosensitive pathway wherein cytoskeletal tension promotes YAP nuclear translocation and downstream transcriptional activity[11]. This mechanosensitive pathway governs YAP/TAZ such that on soft hydrogels or deformable fibrous materials, YAP remains cytosolic, while on stiff hydrogels and in response to stretch, YAP localizes to the nucleus[13]. Given that YAP/TAZ is responsible for mediating most of the downstream functional outcomes of substrate stiffness sensing[6], it is commonly thought of as a mechanical rheostat[6, 14], providing a readout of how a cell is currently processing mechanical inputs from the microenvironment.

In addition to physical cues in the microenvironment, the interactions that cells make with each other also regulate mesenchymal progenitor cell differentiation. For example, in developing limb buds, blockade of cadherin expression limits chondrogenesis, while cadherin overexpression promotes chondrogenesis[15]. Additionally, in mesenchymal stem cells (MSCs) cultured in monolayer, adipogenesis is promoted by cell-cell contact (through high densities), whereas osteogenesis is inhibited by cell-cell contact due to the subsequent decrease in cell-ECM contact area[16]. In mesenchymal cells, cell-cell contact is mediated through the homotypic interaction of N-Cadherin on adjacent cells. N-Cadherin contains both an extracellular domain that mediates this adhesion as well as a cytosolic domain that acts as both a signaling hub and anchor that couples to the actin cytoskeleton[17].

To date, most cadherin mechanobiology has been studied through examination of E-Cadherin and VE-Cadherin in situations where strong adherens junctions form between cells (i.e. early cancer progression, and at epithelial/endothelial cell junctions)[18, 19]. However, despite their strong sequence homology, E-Cadherin and N-Cadherin can show greatly different downstream signaling responses to various stimuli[20]. During mesenchymal development, most of the initial mechanical interactions arise from the formation of adherens junctions within the cell-rich mesenchymal condensation. However, as development progresses, cell-cell interactions are increasingly restricted as progenitor cells differentiate, and subsequently deposit and interact with increasing levels of ECM in the microenvironment[21]. N-Cadherin interactions then become less predominant due to the dense surrounding matrix (Fig. 1a). In accordance with this, the response to the most extracellular N-Cadherin domain (EC1) appears to mediate a large degree of specificity in N-Cadherin adhesion and control over cellular behavior during development[22, 23]. While N-Cadherin has multiple adhesive domains, the addition of short peptide sequences containing

the ‘HAVDI’ adhesive sequence from EC1 inhibits >90% of the N-Cadherin specific response in 3T3 fibroblasts[24], identifying this domain as operative in mediating mesenchymal cell-cell signaling.

Adhesive crosstalk between cadherin-based and integrin-based signaling has previously been found to influence the mechanical state of the cell[25]. This crosstalk can arise at multiple points; N-Cadherin is linked to actin through monomeric α-catenin[26], shares intermediary scaffolding proteins with integrin-based adhesions (e.g. vinculin)[27, 28], and can also control Rho GTPase activity[29]. To query these interactions, several groups have developed platforms to study cell-cell and cell-ECM signaling using micropatterning and other techniques. This includes examining cell doublets on soft hydrogels[30], micropatterning stripes or domains of collagen/fibronectin and cadherin under cells[31, 32], and micropatterning ECM islands that promote cellular interaction[33, 34]. However, these presentation systems are not able to fully decouple adhesive inputs; that is, increased presentation of one signal through increasing domain area (e.g. additional cadherin-patterned culture area) necessitates the reduction in the area of another signal (e.g. cell-ECM patterned area). Additionally, in scenarios where adherens junctions form, additional cell-cell interactions occur (e.g. Nectin and Notch/Delta interactions, as well as paracrine signaling), making interpretation of downstream signaling somewhat convoluted.

An alternative to coated domains of adhesive proteins is the utilization of biomaterials that enable controlled presentation of functional adhesive domains in the form of small peptides ligated to a polymer backbone. The first such example was the short peptide sequence RGD from fibronectin, which enabled cell adhesion to hydrogel surfaces to mimic cell-ECM interactions[35–37]. Building on this approach, our group has recently incorporated ‘HAVDI’ peptides (from N-Cadherin extracellular domain 1, EC1) onto a methacrylated hyaluronic acid (MeHA) backbone. In 3D culture, this modification mimics cell-cell interactions that are important for early chondrogenesis, overcoming a limitation of encapsulation strategies that isolate cells from one another [38]. These MeHA hydrogels also serve as an ideal biomaterial to probe mesenchymal microenvironments, given that the hyaluronic acid backbone itself can promote MSC lineage commitment when compared to purely synthetic hydrogels (e.g., poly(ethylene glycol), PEG)[39].

In this study, we took advantage of the flexibility of the MeHA system to generate a new platform to query how multiple adhesive interactions interact to regulate the functional behavior of MSCs across a range of mechanical microenvironments. To accomplish this, we generated 2D hydrogels that enabled independent co-presentation of both the ‘HAVDI’ adhesive sequence from N-Cadherin (mimicking cell-cell interactions) and the ‘RGD’ adhesive sequence from fibronectin (mimicking cell-ECM interactions), while independently tuning matrix stiffness. Decoupled presentation of these cues demonstrated that HAVDI (in the context of constant RGD) reduced the contractile state and nuclear YAP/TAZ localization in MSCs, resulting in altered interpretation of ECM stiffness and consequent changes in downstream cell proliferation and differentiation. These findings indicate that, in an evolving developmental context, N-Cadherin can alter progenitor cell perception of exogenous biophysical inputs, such as increased ECM stiffness, thereby regulating cell lineage commitment.

Tunable Hydrogels Presenting Cell-Cell and Cell-ECM Ligands

To determine the impact of N-Cadherin adhesive domain presentation on traditional cell-ECM interactions and mechanosensing, we utilized a photopolymerizable methacrylated hyaluronic acid (MeHA) hydrogel system. MeHA hydrogels provide a biologically-active and flexible platform for controlling multiple cellular inputs, such as ligand presentation and hydrogel stiffness. Here, the base MeHA backbone was modified with RGD (from fibronectin) and HAVDI (from N-Cadherin) peptides via a Michael addition reaction of thiols on peptides and methacrylates on MeHA (Fig. 1b). MeHA was modified to levels that formed hydrogels with 1 mM RGD and 1 mM HAVDI included ('*HAVDI/RGD*'), enabling both integrin and cadherin mediated interactions by mesenchymal stem cells (MSCs). Additional hydrogels were modified with 1 mM RGD and 1 mM of a non-functional scrambled HAVDI sequence ('*scram/RGD*') to stimulate integrin-only interactions, while preserving the same level of HA modification and resulting hydrogel mechanical properties. Peptides coupled to the MeHA backbone are present in even amounts throughout the entire hydrogel (Supp. Fig. 1), with peptide surface density of ~1 mM HAVDI, which is on the order of previous measures of E-Cadherin density in developing drosophila embryos and monolayer epithelial cells[40]. Peptide loading at 2 mM (combination of HAVDI and RGD peptides) consumed a very small fraction of available methacrylate groups (~8%). Moreover, the peptide coupling efficiency in this MeHA system (utilizing a cysteine-methacrylate coupling) is quite high, with ~88% of the loaded peptide conjugated to the backbone[38].

Thin MeHA films (thickness ~100 μm) were cast and polymerized onto methacrylated glass coverslips to promote hydrogel adherence. Homogenous peptide loading and localization in MeHA hydrogels was verified through fluorescent peptide tagging and confocal imaging (Supp. Fig. 1). The Young's moduli of hydrogels were determined by AFM, and hydrogels with stiffness values spanning a physiologic range (1–20 kPa) were obtained by increasing the UV exposure time/energy during polymerization (Fig. 1c). Moduli of hydrogels loaded with HAVDI and RGD or with scrambled HAVDI and RGD were not significantly different from one another across the range of exposure times used (Fig. 1c, *inset*). To query preliminary MSC responses to these peptide-coupled substrates, bovine MSCs were seeded onto the hydrogel films for 18 hours. Initial attachment studies with MeHA hydrogels coupled with 1 mM of one peptide (RGD, scrambled HAVDI, HAVDI, or no peptide) were performed to assess the adhesivity of MSCs to hydrogels modified with each single peptide. Non-modified gels or gels loaded with scrambled HAVDI did not support cell attachment. Conversely, when gels were modified with HAVDI alone, cell attachment and spreading was observed (Supp. Fig. 2), albeit at levels much reduced when compared to RGD-conjugated gels (HAVDI attachment ~10% of RGD attachment). This is consistent with previous reports showing that the first two extracellular domains of N-Cadherin (in which the HAVDI sequence resides) allow for weak adhesive interactions when compared to the full ectodomain[41]. Next, we examined 1 mM: 1 mM peptide combinations of HAVDI and RGD across a physiologic range of substrate stiffness, and noted no significant difference in spread area between HAVDI/RGD and scram/RGD groups (Fig. 1c). We additionally observed no differences in cell attachment and spreading between these two material formulations. These observations highlight that cell spreading in this system appears to be

driven by RGD and is not altered by the additional presentation of HAVDI. Additionally, the lack of change in cell spread area with HAVDI presentation shows that the dual-ligand MeHA hydrogel platform permits changes in the presentation of one signal (HAVDI presentation) without changing the availability of the other (RGD presentation and resultant cell spread area).

Staining of external N-Cadherin organization on the basal plane of MSCs on intermediate stiffness MeHA substrates (10 kPa) showed no indication of cadherin clustering as is seen in densely cultured cells (Supp. Fig. 3). Likewise, immunostaining for β-catenin on the basilar plane of the cell showed no distinct structure formation that would indicate clustering with HAVDI presentation (Supp. Fig. 4). Western blotting revealed that HAVDI presentation (in the context of a constant RGD) did not significantly alter N-Cadherin levels after 18h of culture (Supp. Fig. 3). These observations highlight that, on substrates of physiologic stiffness, ligation of 1 mM HAVDI domain does not activate canonical N-Cadherin signaling responses that are seen in dense culture conditions where strong adherens junctions form between cells. Despite this, the EC1 domain containing the HAVDI adhesive sequence has previously been shown to play a critical role in cell sorting and adhesivity in development[42]. Additionally, the HAVDI domain can potently inhibit N-Cadherin responses in fibroblasts *in vitro*[24]. Given that MSCs were able to weakly attach to gels modified with HAVDI peptide alone, we next explored how this domain might regulate MSC mechanosensing within developmental mesenchymal environments with multiple adhesive ligands across a physiologic range of substrate stiffness.

HAVDI Ligation Attenuates YAP/TAZ Mechanosensing

Having established this biomaterial-mediated HAVDI and RGD culture system, we next determined whether downstream mechanosensitive signaling pathways were altered in response to HAVDI ligation with a constant background of RGD ligation. As YAP/TAZ signaling is responsible for many downstream transcriptional outcomes of substrate stiffness sensing, we performed immunostaining for YAP/TAZ (with an antibody that detects both YAP and TAZ in western blotting), and then quantified this staining. YAP/TAZ nuclear-to-cytoplasmic ratios (Fig. 2a) were significantly reduced with HAVDI presentation on intermediate stiffness substrates (10 and 15 kPa) (Fig. 2b). Surprisingly, HAVDI presentation did not significantly alter YAP/TAZ ratios at either the upper or the lower bounds of substrate stiffness investigated (5 or 20 kPa). Sigmoidal curve fits showed "YAP/TAZ_{50}" (LD50 value of curve fit, representing the stiffness at which MSCs had YAP/TAZ ratios of 1.65) values of 6.2 kPa for MSCs on scram/RGD control substrates, which increased to 15.3 kPa on HAVDI/RGD substrates (Fig. 2b). While there was donor-to-donor variability in baseline YAP/TAZ values in these primary cell isolates (likely due to differences in inherent contractility across donors), a similar HAVDI-mediated reduction in nuclear YAP/TAZ was observed across all 12 donors used in this study. Likewise, parallel studies performed with human MSCs showed a similar response, where HAVDI presentation markedly decreased YAP/TAZ nuclear localization at intermediate substrate stiffness (Supp. Fig. 5). Importantly, blocking cellular N-Cadherin with a neutralizing blocking antibody prior to seeding cells on the substrates confirmed that these differences in YAP/TAZ were specific to N-Cadherin driven responses (Fig. 2c).

Given that this MeHA hydrogel system allows for the precise addition of multiple peptides to the HA backbone, we next established the dose-dependence of HAVDI presentation on this mechanosensing response. For this, the standard 1:1 ratio of RGD to HAVDI peptide was titrated with increasing levels of functional HAVDI peptide (Fig. 2d). Visualization and quantification of YAP/TAZ ratios showed a strong dose dependence with HAVDI peptide presentation, such that for a given substrate stiffness, increasing amounts of functional HAVDI resulted in lower YAP/TAZ nuclear-to-cytoplasmic ratios (Fig. 2e–f).

Next, a competition study was performed to determine if adding soluble HAVDI peptide to the culture media would abrogate this YAP/TAZ response. Addition of 1 mM of scrambled peptide did not significantly alter the YAP/TAZ response from control values in either material group, whereas addition of 1mM soluble HAVDI peptide completely abrogated the response to HAVDI/RGD presentation (Fig. 2g). Importantly, adding this soluble HAVDI to MSCs on control scram/RGD substrates did not lower YAP/TAZ ratios (Fig. 2g), indicating that HAVDI peptides need to be tethered in order to elicit reductions in YAP/TAZ nuclear localization. This is in accordance with recent studies showing the importance of force acting through cadherin-cadherin adhesion in regulating certain regimes of cytosolic cadherin signaling, such as modulating β-catenin to actin binding[43], opening α-catenin cryptic binding domains[44], and activating RhoGAPs[45].

Noting that differences in nuclear YAP/TAZ accumulation can lead to alterations in functional behavior, we next determined whether HAVDI presentation altered important stem cell behaviors such as differentiation and proliferation. To examine MSC differentiation in this developmental context, we assayed early osteogenic lineage commitment in individual cells through via RUNX2 nuclear localization (which activates ALP expression and regulates osteogenesis) following osteoinduction. After one day of culture in growth media there were low levels of nuclear RUNX2 in MSCs cultured on either substrate (Fig. 2g–h, Supp. Fig. 6). However, after two days of osteogenic induction, MSCs on HAVDI/RGD hydrogels showed greatly reduced nuclear RUNX2 levels compared to MSCs on scram/RGD hydrogels, indicating less osteogenic commitment following HAVDI ligation. Other functional outcomes of nuclear YAP/TAZ localization were also altered; MSC proliferation was reduced by ~35% of baseline values following 48 hours of culture on HAVDI-modified hydrogels (Fig. 2i).

One other aspect important to N-Cadherin action during development is its temporal presentation and activity, which is regulated both by cell-cell interaction and the expression of proteases that cleave the N-Cadherin ectodomain. ADAM10 (A Disintegrin and Metalloproteinase 10) is expressed during development of mesenchymal tissues, and its action (in part) is to cleave external type-1 cadherin domains. Indeed, several studies have specifically highlighted how ADAM10 cleavage of the extracellular domain of N-Cadherin is essential for early limb development and chondrogenesis (*Nakazora+, BBRC*, 2010). To investigate how HAVDI-attenuated ECM mechanosensing may be regulated throughout development, we performed an experiment wherein recombinant ADAM10 was added to MSCs that had been cultured on 10 kPa scram/RGD and HAVDI/RGD substrates. Treatment with recombinant ADAM10 had no effect on MSCs cultured on control scram/RGD substrates (Supp. Fig. 7). Conversely, addition of ADAM10 completely abrogated the

response of MSCs to HAVDI/RGD substrates, returning YAP/TAZ ratios back to baseline levels. This illustrates that HAVDI-altered mechanosensing may be countermanded by increased expression of ADAM10 during development, allowing for downstream lineage commitment to proceed. Taken together, this data suggests that HAVDI/N-Cadherin ligation, and its temporal regulation, may be an important determinant of MSC fate commitment during mesenchymal development.

Given that YAP/TAZ governs many downstream outcomes of substrate stiffness sensing, our data suggests that HAVDI ligation leads to an altered interpretation of substrate stiffness. Across an intermediate stiffness range, MSCs cultured on HAVDI/RGD substrates showed lowered YAP/TAZ nuclear localization on a given stiffness compared to cells on scram/RGD substrates. For example, MSCs on softer scram/RGD substrates (E=5 kPa) promoting only cell-ECM interactions exhibited the same YAP/TAZ ratios as the same cell population on a much stiffer (E=15 kPa) substrate promoting both cell-cell and cell-ECM interactions. As such, signaling from HAVDI appears to “override” the mechanosensitive YAP/TAZ signaling that results from RGD-integrin (cell-ECM) stiffness sensing. Interestingly, cells on HAVDI/RGD hydrogels do eventually increase in YAP/TAZ nuclear localization, but they do so at a higher substrate stiffness, suggesting that HAVDI ligation acts as a signaling offset while preserving the ability of MSCs to eventually sense increases in ECM stiffness. At both the upper and lower bounds of substrate stiffness probed, there was no difference in YAP/TAZ signaling with HAVDI, indicating that the mechanism driving this altered interpretation is not functional at these boundaries. Finally, these alterations in YAP/TAZ localization through HAVDI ligation were sufficient to shift functional behavior of stem cells at a given substrate stiffness, promoting lineage pathway commitment and proliferation regimes that would otherwise preferentially occur in a different mechanical niche. Taken together, these data show that N-Cadherin/HAVDI signals act to offset ECM-driven YAP/TAZ signaling in MSCs.

HAVDI Ligation Reduces MSC Contractility

Based on the aforementioned alterations in downstream mechanosensitive signaling, we next set out to determine if N-Cadherin ligation of the HAVDI adhesive sequence alters YAP/TAZ signaling through altering the contractile state of the cell. To accomplish this, we examined how multiple components of the actin cytoskeleton changed in response to simultaneous presentation of HAVDI and RGD on 10 kPa substrates. Confocal z-stacks of F-actin showed that cells plated on intermediate stiffness (10 kPa) scram/RGD substrates exhibited prominent F-actin organization and alignment, with highly organized apical stress fibers and a more aligned basilar plane (Fig. 3a, Supp. Fig. 8). Conversely, cells on HAVDI/RGD substrates had significantly reduced organization of F-actin structures (quantified as the F-actin anisotropy ratio) in both the apical and basilar planes. Paxillin immunostaining was also performed to visualize focal adhesions (FAs) in cells on scram/RGD and HAVDI/RGD substrates. Analysis of the number of FA showed no difference between substrates; however, FA area, aspect ratio, and length all decreased on HAVDI/RGD compared to control hydrogels (Fig. 3b, Supp. Fig. 9). Further analysis of the FA populations showed that HAVDI/RGD interaction led to a significant depletion of the large FA fraction (Supp. Fig. 10). To determine how these changes in the cytoskeleton

altered how cells were mechanically probing and deforming their extracellular environment, traction force microscopy was performed. Results from this assay showed that presentation of HAVDI (along with RGD) on 10 kPa substrates resulted in a ~50% decrease in traction stress generation (Fig. 3c).

Taken together, these data suggest that the ligation of the HAVDI domain from N-Cadherin alters the ability of MSCs to mechanically probe their microenvironment. Reduced actin organization and reduced FA size when cell-cell and cell-ECM ligands were simultaneously presented at a 1:1 ratio are both indicative of the reduced contractility in cell-ECM interactions[8]. Of note, these changes in contractility occurred independently of canonical relationships between traction and spreading, as the reduced traction force occurred without significant differences in the spread cell area. As such, HAVDI ligation is able to reduce the contractile state of the cell and can perturb the ability of an MSC to generate contractile forces and deform the underlying substrate, altering the interpretation of substrate stiffness cues via the mechanosensitive YAP/TAZ pathway.

HAVDI Ligation alters MSC Mechanosensing via Rac1/MyosinIIA

Based on the above, we next sought to determine the mechanism by which HAVDI peptide presentation alters the mechanical state of cells on these intermediate stiffness hydrogels. Given that N-Cadherin serves as a signaling hub for multiple Rho GTPases (RhoA, Rac1), we tested these pathways in terms of their regulation of the YAP/TAZ response to 10 kPa HAVDI/RGD hydrogels. First, NSC-23766 was used to inhibit Rac1 activity and Y-27632 was used to inhibit downstream Rho kinase activity (ROCK). Both inhibitors were added for 1 hour before analysis. Blocking Rac1 with NSC-23766 completely abrogated any differences in YAP/TAZ nuclear localization between groups. Conversely, blocking ROCK activity with Y-27632 lowered the overall YAP/TAZ signal in both groups, while maintaining the significant differences in localization with HAVDI presentation (Fig. 4a). Treatment with both inhibitors had an additive effect, with overall levels of YAP/TAZ signaling decreasing and no differences observed in YAP/TAZ nuclear localization. These Rho and Rac pathway perturbations did not significantly alter the spread cell area between MSCs on scram/RGD hydrogels and on HAVDI/RGD hydrogels (Supp. Fig. 11).

When Rac1 activity was inhibited, we noted that the average YAP/TAZ localization on the HAVDI/RGD hydrogels did not significantly change, but rather that the YAP/TAZ ratios dropped significantly in MSCs on the control scram/RGD substrates. This suggested that the this HAVDI motif from N-Cadherin might already be acting to block Rac1 activity in MSCs prior to pharmacological inhibition with NSC-23766. This would be consistent with other findings of lowered Rac1 activation levels after N-Cadherin contact[46, 47]. To confirm that this was the case, we transduced MSCs with adenoviral constructs containing a constitutively active (CA) version of Rac1[33] and monitored YAP/TAZ signaling. Compared to untreated and LacZ transduced controls, CA Rac1 rescued YAP/TAZ signaling in MSCs on HAVDI/RGD hydrogels, restoring levels to that observed on control hydrogels (Fig. 4b). Overall, these findings support the notion that HAVDI presentation acts to inhibit Rac1 activation, which thereby leads to altered MSC YAP/TAZ mechanosensing through alterations in the mechanical state of the cell.

Next, we sought to understand what pathways Rac1 was controlling in order to alter the mechanical state of the cell, and why this mechanism was only operative at intermediate matrix elasticities. It is unlikely that canonical mechanosensitive N-Cadherin signaling is responsible for these reductions on intermediate stiffness substrates, as treatment with Y27 (which inhibits ROCK and lowers contractility) lowered overall YAP/TAZ levels while preserving the HAVDI mediated reductions in nucear YAP/TAZ (Fig. 4a). In previous work, we showed that mechanosensitive mediators of substrate stiffness sensing in focal adhesions (FAK, p130Cas) could interact with and control Rac1 activation, altering cellular stiffening and controlling N-Cadherin expression[34, 48]. Western blotting showed that mechanosensitive focal adhesion proteins that normally have increased expression or activation with increased substrate stiffness (pFAK, p130Cas) were not differentially activated/expressed in MSCs cultured on 10 kPa scram/RGD or HAVDI/RGD hydrogels (Supp. Fig. 12). Additionally, it has been shown that actin-bundling proteins downstream of Rac1, such as cofilin, can control YAP/TAZ localization[10]. Consistent with these reports, pCofilin levels decreased with HAVDI presentation, though this response was of a small magnitude and it is unclear if this expression is upstream or downstream of actin organizational cues (Supp. Fig. 12).

Another possible mechanism through which Rac1 could alter the mechanical state of the cell was recently elucidated in a study which showed that Rac1-GTP can increase the accumulation of Myosin-IIA in focal adhesions, therein modulating their size and maturation, as well as downstream functional consequences of FA assembly such as cell migration[49]. In this mechanism, active Rac1 was found to control the phosphorylation of a specific residue on Myosin-IIA (S1916), promoting Myosin-IIA's capture in focal adhesions and increasing their maturation and growth. Importantly for our work, p1916 residue phosphorylation (that regulates the capture) was found to be highest in cells on intermediate stiffness substrates (8.6 kPa), with p1916 phosphorylation being similarly low on both upper/lower bounds of ECM stiffness (55 kPa and 0.7 kPa, respectively).

To determine if this mechanism was operative in the HAVDI-mediated attenuation of mechanosensing that we observed, we quantified the amount of Myosin-IIA in focal adhesions utilizing the same computational methods as originally described in this work[49]. MSCs cultured on 10 kPa HAVDI/RGD hydrogels had lower levels of Myosin-IIA in focal adhesions, with a ~35% reduction in the percentage of focal adhesion area positive for myosin-IIA compared to scram/RGD controls, a reduction that is consistent with previously reported myosin-IIA incorporation levels between cells transduced with constitutively active (CA) and dominant negative (DN) Rac1 vectors (Fig. 4c–d). Additionally, the original description of this mechanism showed that myosin-IIA phosphorylation and FA incorporation was mediated by PKCβII activity. To that end, we treated MSCs on 10 kPa hydrogels with LY-333531, a highly specific isozyme-selective pharmacological inhibitor of PKCβII (reported IC_{50}= 6 nM). Consistent with this Rac1/MIIA mechanism being active, treatment with this inhibitor resulted in the complete abrogation of any differences in YAP/TAZ localization with HAVDI presentation, in a dose-dependent manner (Fig. 4e). These changes occurred in MSCs cultured on scram/RGD substrates but did not significantly alter YAP/TAZ ratios of MSCs cultured on HAVDI/RGD substrates, likely due to the fact that the Rac1 activity that governs this mechanism is already low in MSCs on these

HAVDI/RGD substrates. Taken together, these findings indicate that this Rac1 mechanism likely controls the HAVDI-mediated attenuation of ECM mechanosensing by MSCs.

Importantly, the implication of this Rac1-MyosinIIA mechanism in HAVDI-mediated attenuation of ECM mechanosensing helps to explicate why this phenomenon only occurred at an intermediate stiffness (Fig. 2b). Rac1 has previously been found to play a role in establishing the contractile state of the cell, with cellular elastic moduli decreasing similarly when treated with Y27 (-ROCK) or NSC (-Rac1 activation) on intermediate stiffness substrates[34]. This data mirrors our YAP/TAZ data after blocking with Y27 or NSC (Fig. 4A), and suggests that there is a baseline decline in contractile state that arises from reduced Rac1 activity, which likely stems from Rac1-GTP's ability to control actin organization and dynamics through mediators such as Arp2/3 and cofilin[50]. While the precise molecular mediator between HAVDI/N-Cadherin and subsequent Rac1 activation is unclear, previous studies have demonstrated numerous potential pathways though which cadherins can coordinate Rho-GTPase activation, including the suppression of Rac1 activity[46, 47, 51, 52]. Our data examining the involvement of Rac1 activity and Myosin-IIA localization suggests that there is enough contractile energy in MSCs on scram/RGD substrates at the intermediate stiffness to initiate the Rac1-controlled Myosin-IIA recruitment into the FA (Fig. 4c–e), thereby increasing the contractile state of the cell. However, when HAVDI interactions are introduced, the subsequent reduction of Rac1-GTP lowers the contractile state of the cell (Fig. 4a–b) and thereby necessitates additional contractile energy (initiated by increased matrix elasticity) before initiate downstream signaling is initiated. To further determine the importance of this Rac1 mechanism in driving the mechanical response to HAVDI ligation, we cultured MSCs on HAVDI/RGD and scram/RGD substrates of varying stiffness and inhibited Rac1 activity with NSC-23766. Consistent with the inability of this Rac1 mechanism to operate at lower/higher boundaries of substrate stiffness, we found no significant differences in YAP/TAZ nuclear localization with HAVDI presentation on 5 or 20 kPa stiffness substrates following NSC treatment (Supp. Fig. 13). Taken together, these studies show that the HAVDI-mediated alterations in the contractile state of the actin cytoskeleton at an intermediate stiffness is the result of reduced Rac1 activation and the subsequent reduction of Myosin-IIA localization into focal adhesions. More broadly, these data suggest an important role for Rac1 in regulating context-specific changes in mechanosensing of progenitor cells residing within complex developmental microenvironments.

Outlook

This work developed a hyaluronic acid hydrogel platform to enable fully decoupled and modular presentation of cell-cell and cell-ECM adhesive interactions in order to provide new insight into how these inputs summate to regulate stem cell mechanosensing in complex developmental mesenchymal microenvironments. Using this platform, we elucidated a novel mechanobiological mechanism that emerges as a consequence of diverse adhesive interactions (Fig. 5). Specifically, we found that biologically-meaningful epitopes present during mesenchymal development can alter intrinsic force sensing mechanisms and set points to regulate progenitor cell perception of the microenvironment. In this mechanism, ligation of the HAVDI adhesive domain from N-Cadherin EC1 (in the context of constant

RGD ligand) led to Rac1-GTP dependent reductions in the capture of Myosin-IIA into focal adhesions. This lack of Myosin-IIA incorporated into focal adhesions hindered the maturation of these adhesions with increasing substrate stiffness, and thereby decreased traction force generation on the underlying substrate. These alterations in the mechanical state of the cell reduced mechanosensitive YAP/TAZ translocation to the nucleus, thereby attenuating stem cell behaviors important for mesenchymal development, including proliferation and osteogenic differentiation. Collectively, these data establish that, in some physiologic environments, N-Cadherin ligation can “shield” the cell from the interpretation of exogenous ECM stiffness cues by limiting the contractile state of the cell.

More generally, this work highlights how the MSC response to biophysical inputs can be confounded by other signals present in the complex and time-evolving microenvironments in which they reside. To date, most of the literature on cadherin mechanobiology has focused on E-Cadherin/VE-Cadherin within niches where there is strong adherens junction formation between cells. However, during mesenchymal development, cadherin based cell-cell interactions are increasingly restricted and reduced as progenitor cells deposit ECM and interact with their microenvironment[21]. Given this, during the dynamic process of limb development, HAVDI/N-Cadherin mediated alteration in ECM mechanosensing likely represents an important regulator of tissue maturation, where it would function to prevent ECM signals from initiating or altering lineage specification too early in development. Mechanistically, this could be important in tissue patterning, where matrix accumulation and maturation could occur until such time as the “shielding” mediated by HAVDI is overcome, culminating in commitment to the fully-differentiated phenotype. HAVDI-mediated regulation of ECM mechanosensing may also be relevant in pathologies that disrupt the balance of cell-ECM and cell-cell signaling, such as fibrosis and wound healing. While this data illustrates that HAVDI and N-Cadherin adhesion contribute to mechanosensing, the role of this mechanism in the complex and time evolving *in vivo* microenvironment remains to be determined. However, just as the RGD adhesive domain from fibronectin has proven to be a valuable tool for studying many aspects of cell-ECM adhesion and signaling, so too might the incorporation of the HAVDI adhesive domain of N-Cadherin be a useful tool in studying the influence of cell-cell adhesion and signaling in engineered microenvironments. These results suggest that HAVDI presentation may be further harnessed towards novel biomaterial design to direct mesenchymal stem cell behavior and for tuning of the cellular response to substrate stiffness in regenerative medicine applications.

Materials and Methods

Methacrylated Hyaluronic Acid (MeHA) Hydrogel Synthesis and Casting

MeHA was synthesized as previously reported[53], where methacrylic anhydride was reacted with 1% w/v sodium hyaluronate (70 kDa, Lifecore Biosciences) in dH2O with pH maintained at 8 ± 0.5. After reacting for 6h, the macromer solution was purified via dialysis (MW cutoff of 6–8 kDa) and then lyophilized for storage. Methacrylation level was confirmed to be ~31% by ^{1}H NMR (Supp. Fig. 14). Small peptide sequences (Genscript) from adhesive domains for fibronectin (GCGYG**RGD**SPG), N-cadherin (Ac-**HAVDI**GGGC), or a scrambled N-Cadherin control (Ac-AGVGDHIGC) were covalently

conjugated to the HA backbone via Michael-type addition reactions of the cysteine residues on these peptides with the methacrylate on the HA backbone. Peptide coupling occurred overnight at 37°C in TEA buffer (pH 8, Sigma). For these studies, all peptides were added for final hydrogel concentrations of 1 mM. Thin hydrogel films (thickness = 100 μm) of 3% w/v MeHA were cast and polymerized on methacrylated glass coverslips (as in [54]) that allowed for covalent attachment of the MeHA hydrogel to the coverslip hydrogel during UV polymerization. Irgacure-2959 was added to this MeHA precursor solution at a final concertation of 0.05% v/v and then polymerized using a UV polymerization box with an output of 4.5 mW/cm^2 at a wavelength of 365nm. Varied polymerization times were used to alter hydrogel mechanics.

Cell Isolation, Culture, and Pharmacologic Inhibition

Juvenile bovine MSCs were harvested from tibio-femoral bone marrow as previously described by Huang et al[55]. All MSCs were cultured in standard growth media (HG-DMEM, 10% fetal bovine serum (FBS), and 1% penicillin, streptomycin, Fungizone (PSF)) for all experiments, and were cultured on tissue culture plastic (TCP) for one passage prior to re-plating on the MeHA substrates. Osteogenic induction media (growth media with 0.1 μM dexamethasone, 50 mg/mL ascorbate-2-phosphate, and 10 mM β-glycerophosphate) was used for assaying the MSC osteogenic differentiation capability. For substrate studies, cells were seeded at a density of 3,000 cells/cm^2 to prevent cell-cell interactions. Once seeded, MSCs were cultured on MeHA hydrogels for 18 hrs before subsequent fixation. Pharmacologic inhibition of Rac1 activity was achieved using 50 μM NSC-23766 (Tocris Bioscience #2161), inhibition of ROCK was achieved using 10 μM Y-27632 (Calbiochem #688000), and inhibition of was achieved using 50/200 nM LY-333531 (Tocris Bioscience #4738). Inhibitors were added into the culture media for one hour prior to fixation and subsequent analyses. N-Cadherin blocking was accomplished by adding a neutralizing N-Cadherin antibody (50 μg/mL, Sigma #GC4) to trypsinized cells in growth media for 45 min at 4°C before 2X PBS rinses, spin down, and reseeding onto culture substrates. Soluble peptide competition studies were performed by adding 1 mM of peptide (either scrambled or HAVDI) to the growth media directly following seeding. For ADAM10 studies, mouse recombinant ADAM10 (R&D Systems #946-AD-020) was added to culture media at 100 ng/mL for 4 hours prior to fixation and subsequent analysis.

Immunostaining and Quantification of YAP/TAZ Localization

For normal immunostaining, MSCs were fixed in room temperature 4% PFA for 18 min, and then washed three times with PBS, followed by 10 min permeabilization at 4°C with 0.05% Triton X-100 in PBS supplemented with 320 mM sucrose and 6 mM magnesium chloride. To enable analysis of focal adhesions, soluble intracellular components were removed via fixation in a microtubule stabilization buffer for 10 min at 37°C. Primary antibodies were diluted in 1% BSA in PBS and added overnight at 4°C. Antibodies and dilutions used in this study included anti-YAP (1:200; Santa Cruz #sc-101199), anti-β-catenin (1:500; Cell Signaling #8480), anti-N-cadherin (1:400; Santa Cruz #9379, #59987), anti-RUNX2 (1:250; Abcam #76956), anti-paxillin (1:500, BD #610052), anti-myosin-IIA (1:400, Abcam #24762). After three PBS rinses, AlexaFluor-488/546 [H+L] secondary antibodies (Molecular Probes) were added for 1hr at room temperature. F-Actin staining was performed

using AlexaFluor-conjugated phallodiin (1:1000; Molecular Probes #A22283) added in with the secondary antibodies and incubated for 1hr at room temperature. Following this incubation, three additional PBS rinses were followed by DAPI staining and mounting using ProLong Gold AntiFade (Life Technologies #P36935). Images were taken on a Nikon A1R Confocal Microscope at 60x 1.4 NA (0.41 μm/px). Proliferation was assayed through the Click-IT EdU Immunostaining kit (Invitrogen). YAP/TAZ ratios were quantified through imaging of YAP/TAZ staining with a pinhole diameter of 51.09 μm (1.6 AU). Nuclear images were utilized to delineate the nuclear area from the cytoplasmic region of the cell, and the average fluorescent intensity over each region was calculated using ImageJ as in[13].

Statistical Analysis

All experiments were performed using 2–3 MSC donors and at least 3 replicate hydrogels per condition. Statistical comparisons were performed using an independent sample t-test when only two groups were being compared, and one- or two-way analysis of variance (ANOVA) with Bonferroni's post hoc testing used to make pairwise comparisons between multiple groups. Statistical significance was set to $p < 0.05$.

Supplementary Material

Refer to Web version on PubMed Central for supplementary material.

Acknowledgments

The authors would like to thank Ms. Claire McLeod for assistance with Atomic Force Microscopy and curve fitting, Mr. Chris Rodell for helpful discussions regarding MeHA synthesis and peptide conjugation, and Dr. Murat Guvendiren for assistance with preliminary studies. This work was funded by the National Institutes of Health (R01 EB008722, R01 HL115553) and the Penn Center for Musculoskeletal Disorders (P30 AR050950).

References

1. Cameron AR, Frith JE, Cooper-White JJ. The influence of substrate creep on mesenchymal stem cell behaviour and phenotype. Biomaterials. 2011; 32(26):5979–5993. [PubMed: 21621838]
2. Engler AJ, Sen S, Sweeney HL, Discher DE. Matrix elasticity directs stem cell lineage specification. Cell. 2006; 126(4):677–689. [PubMed: 16923388]
3. Guvendiren M, Burdick JA. Stiffening hydrogels to probe short- and long-term cellular responses to dynamic mechanics. Nat Commun. 2012; 3:792. [PubMed: 22531177]
4. Huebsch N, Arany PR, Mao AS, Shvartsman D, Ali OA, Bencherif SA, et al. Harnessing traction-mediated manipulation of the cell/matrix interface to control stem-cell fate. Nat Mater. 2010; 9(6): 518–526. [PubMed: 20418863]
5. Khetan S, Guvendiren M, Legant WR, Cohen DM, Chen CS, Burdick JA. Degradation-mediated cellular traction directs stem cell fate in covalently crosslinked three-dimensional hydrogels. Nat Mater. 2013; 12(5):458–465. [PubMed: 23524375]
6. Yang C, Tibbitt MW, Basta L, Anseth KS. Mechanical memory and dosing influence stem cell fate. Nat Mater. 2014; 13(6):645–652. [PubMed: 24633344]
7. Geiger B, Spatz JP, Bershadsky AD. Environmental sensing through focal adhesions. Nat Rev Mol Cell Biol. 2009; 10(1):21–33. [PubMed: 19197329]
8. Fu J, Wang YK, Yang MT, Desai RA, Yu X, Liu Z, et al. Mechanical regulation of cell function with geometrically modulated elastomeric substrates. Nat Methods. 2010; 7(9):733–736. [PubMed: 20676108]

9. Wozniak MA, Desai R, Solski PA, Der CJ, Keely PJ. ROCK-generated contractility regulates breast epithelial cell differentiation in response to the physical properties of a three-dimensional collagen matrix. J Cell Biol. 2003; 163(3):583–595. [PubMed: 14610060]
10. Aragona M, Panciera T, Manfrin A, Giulitti S, Michielin F, Elvassore N, et al. A mechanical checkpoint controls multicellular growth through YAP/TAZ regulation by actin-processing factors. Cell. 2013; 154(5):1047–1059. [PubMed: 23954413]
11. Dupont S, Morsut L, Aragona M, Enzo E, Giulitti S, Cordenonsi M, et al. Role of YAP/TAZ in mechanotransduction. Nature. 2011; 474(7350):179–183. [PubMed: 21654799]
12. Gumbiner BM, Kim NG. The Hippo-YAP signaling pathway and contact inhibition of growth. J Cell Sci. 2014; 127(Pt 4):709–717. [PubMed: 24532814]
13. Driscoll TP, Cosgrove BD, Heo SJ, Shurden ZE, Mauck RL. Cytoskeletal to Nuclear Strain Transfer Regulates YAP Signaling in Mesenchymal Stem Cells. Biophys J. 2015; 108(12):2783–2793. [PubMed: 26083918]
14. Low BC, Pan CQ, Shivashankar GV, Bershadsky A, Sudol M, Sheetz M. YAP/TAZ as mechanosensors and mechanotransducers in regulating organ size and tumor growth. FEBS Lett. 2014; 588(16):2663–2670. [PubMed: 24747426]
15. Delise AM, Tuan RS. Analysis of N-cadherin function in limb mesenchymal chondrogenesis in vitro. Dev Dyn. 2002; 225(2):195–204. [PubMed: 12242719]
16. McBeath R, Pirone DM, Nelson CM, Bhadriraju K, Chen CS. Cell shape, cytoskeletal tension, and RhoA regulate stem cell lineage commitment. Dev Cell. 2004; 6(4):483–495. [PubMed: 15068789]
17. Gumbiner BM. Regulation of cadherin-mediated adhesion in morphogenesis. Nat Rev Mol Cell Biol. 2005; 6(8):622–634. [PubMed: 16025097]
18. Lecuit T, Yap AS. E-cadherin junctions as active mechanical integrators in tissue dynamics. Nat Cell Biol. 2015; 17(5):533–539. [PubMed: 25925582]
19. Wei SC, Fattet L, Tsai JH, Guo Y, Pai VH, Majeski HE, et al. Matrix stiffness drives epithelial-mesenchymal transition and tumour metastasis through a TWIST1-G3BP2 mechanotransduction pathway. Nat Cell Biol. 2015; 17(5):678–688. [PubMed: 25893917]
20. El Sayegh TY, Kapus A, McCulloch CA. Beyond the epithelium: cadherin function in fibrous connective tissues. FEBS Lett. 2007; 581(2):167–174. [PubMed: 17217950]
21. Kalson NS, Lu Y, Taylor SH, Starborg T, Holmes DF, Kadler KE. A structure-based extracellular matrix expansion mechanism of fibrous tissue growth. Elife. 2015; 4
22. Patel SD, Ciatto C, Chen CP, Bahna F, Rajebhosale M, Arkus N, et al. Type II cadherin ectodomain structures: implications for classical cadherin specificity. Cell. 2006; 124(6):1255–1268. [PubMed: 16564015]
23. Price SR, De Marco Garcia NV, Ranscht B, Jessell TM. Regulation of motor neuron pool sorting by differential expression of type II cadherins. Cell. 2002; 109(2):205–216. [PubMed: 12007407]
24. Williams E, Williams G, Gour BJ, Blaschuk OW, Doherty P. A novel family of cyclic peptide antagonists suggests that N-cadherin specificity is determined by amino acids that flank the HAV motif. J Biol Chem. 2000; 275(6):4007–4012. [PubMed: 10660557]
25. Weber GF, Bjerke MA, DeSimone DW. Integrins and cadherins join forces to form adhesive networks. J Cell Sci. 2011; 124(Pt 8):1183–1193. [PubMed: 21444749]
26. Desai R, Sarpal R, Ishiyama N, Pellikka M, Ikura M, Tepass U. Monomeric alpha-catenin links cadherin to the actin cytoskeleton. Nat Cell Biol. 2013; 15(3):261–273. [PubMed: 23417122]
27. le Duc Q, Shi Q, Blonk I, Sonnenberg A, Wang N, Leckband D, et al. Vinculin potentiates E-cadherin mechanosensing and is recruited to actin-anchored sites within adherens junctions in a myosin II-dependent manner. J Cell Biol. 2010; 189(7):1107–1115. [PubMed: 20584916]
28. Twiss F, Le Duc Q, Van Der Horst S, Tabdili H, Van Der Krogt G, Wang N, et al. Vinculin-dependent Cadherin mechanosensing regulates efficient epithelial barrier formation. Biol Open. 2012; 1(11):1128–1140. [PubMed: 23213393]
29. Ratheesh A, Priya R, Yap AS. Coordinating Rho and Rac: the regulation of Rho GTPase signaling and cadherin junctions. Prog Mol Biol Transl Sci. 2013; 116:49–68. [PubMed: 23481190]

30. Maruthamuthu V, Sabass B, Schwarz US, Gardel ML. Cell-ECM traction force modulates endogenous tension at cell-cell contacts. Proc Natl Acad Sci U S A. 2011; 108(12):4708–4713. [PubMed: 21383129]
31. Borghi N, Lowndes M, Maruthamuthu V, Gardel ML, Nelson WJ. Regulation of cell motile behavior by crosstalk between cadherin- and integrin-mediated adhesions. Proc Natl Acad Sci U S A. 2010; 107(30):13324–13329. [PubMed: 20566866]
32. Tsai J, Kam L. Rigidity-dependent cross talk between integrin and cadherin signaling. Biophys J. 2009; 96(6):L39–41. [PubMed: 19289031]
33. Liu Z, Tan JL, Cohen DM, Yang MT, Sniadecki NJ, Ruiz SA, et al. Mechanical tugging force regulates the size of cell-cell junctions. Proc Natl Acad Sci U S A. 2010; 107(22):9944–9949. [PubMed: 20463286]
34. Mui KL, Bae YH, Gao L, Liu SL, Xu T, Radice GL, et al. N-Cadherin Induction by ECM Stiffness and FAK Overrides the Spreading Requirement for Proliferation of Vascular Smooth Muscle Cells. Cell Rep. 2015
35. Burdick JA, Anseth KS. Photoencapsulation of osteoblasts in injectable RGD-modified PEG hydrogels for bone tissue engineering. Biomaterials. 2002; 23(22):4315–4323. [PubMed: 12219821]
36. Pierschbacher MD, Ruoslahti E. Cell attachment activity of fibronectin can be duplicated by small synthetic fragments of the molecule. Nature. 1984; 309(5963):30–33. [PubMed: 6325925]
37. Yamada KM, Kennedy DW. Dualistic nature of adhesive protein function: fibronectin and its biologically active peptide fragments can autoinhibit fibronectin function. J Cell Biol. 1984; 99(1 Pt 1):29–36. [PubMed: 6736130]
38. Bian L, Guvendiren M, Mauck RL, Burdick JA. Hydrogels that mimic developmentally relevant matrix and N-cadherin interactions enhance MSC chondrogenesis. Proc Natl Acad Sci U S A. 2013; 110(25):10117–10122. [PubMed: 23733927]
39. Chung C, Burdick JA. Influence of three-dimensional hyaluronic acid microenvironments on mesenchymal stem cell chondrogenesis. Tissue Eng Part A. 2009; 15(2):243–254. [PubMed: 19193129]
40. Truong Quang BA, Mani M, Markova O, Lecuit T, Lenne PF. Principles of E-cadherin supramolecular organization in vivo. Curr Biol. 2013; 23(22):2197–2207. [PubMed: 24184100]
41. Fichtner D, Lorenz B, Engin S, Deichmann C, Oelkers M, Janshoff A, et al. Covalent and density-controlled surface immobilization of E-cadherin for adhesion force spectroscopy. PLoS One. 2014; 9(3):e93123. [PubMed: 24675966]
42. Halbleib JM, Nelson WJ. Cadherins in development: cell adhesion, sorting, and tissue morphogenesis. Genes Dev. 2006; 20(23):3199–3214. [PubMed: 17158740]
43. Buckley CD, Tan J, Anderson KL, Hanein D, Volkmann N, Weis WI, et al. Cell adhesion. The minimal cadherin-catenin complex binds to actin filaments under force. Science. 2014; 346(6209): 1254211. [PubMed: 25359979]
44. Yonemura S, Wada Y, Watanabe T, Nagafuchi A, Shibata M. alpha-Catenin as a tension transducer that induces adherens junction development. Nat Cell Biol. 2010; 12(6):533–542. [PubMed: 20453849]
45. Yang B, Radel C, Hughes D, Kelemen S, Rizzo V. p190 RhoGTPase-activating protein links the beta1 integrin/caveolin-1 mechanosignaling complex to RhoA and actin remodeling. Arterioscler Thromb Vasc Biol. 2011; 31(2):376–383. [PubMed: 21051664]
46. Charrasse S, Meriane M, Comunale F, Blangy A, Gauthier-Rouviere C. N-cadherin-dependent cell-cell contact regulates Rho GTPases and beta-catenin localization in mouse C2C12 myoblasts. J Cell Biol. 2002; 158(5):953–965. [PubMed: 12213839]
47. Ouyang M, Lu S, Kim T, Chen CE, Seong J, Leckband DE, et al. N-cadherin regulates spatially polarized signals through distinct p120ctn and beta-catenin-dependent signalling pathways. Nat Commun. 2013; 4:1589. [PubMed: 23481397]
48. Bae YH, Mui KL, Hsu BY, Liu SL, Cretu A, Razinia Z, et al. A FAK-Cas-Rac-lamellipodin signaling module transduces extracellular matrix stiffness into mechanosensitive cell cycling. Sci Signal. 2014; 7(330):ra57. [PubMed: 24939893]

49. Pasapera AM, Plotnikov SV, Fischer RS, Case LB, Egelhoff TT, Waterman CM. Rac1-dependent phosphorylation and focal adhesion recruitment of myosin IIA regulates migration and mechanosensing. Curr Biol. 2015; 25(2):175–186. [PubMed: 25544611]
50. Jaffe AB, Hall A. Rho GTPases: biochemistry and biology. Annu Rev Cell Dev Biol. 2005; 21:247–269. [PubMed: 16212495]
51. Watanabe T, Sato K, Kaibuchi K. Cadherin-mediated intercellular adhesion and signaling cascades involving small GTPases. Cold Spring Harb Perspect Biol. 2009; 1(3):a003020. [PubMed: 20066109]
52. Wildenberg GA, Dohn MR, Carnahan RH, Davis MA, Lobdell NA, Settleman J, et al. p120-catenin and p190RhoGAP regulate cell-cell adhesion by coordinating antagonism between Rac and Rho. Cell. 2006; 127(5):1027–1039. [PubMed: 17129786]
53. Burdick JA, Chung C, Jia X, Randolph MA, Langer R. Controlled degradation and mechanical behavior of photopolymerized hyaluronic acid networks. Biomacromolecules. 2005; 6(1):386–391. [PubMed: 15638543]
54. Marklein RA, Burdick JA. Spatially controlled hydrogel mechanics to modulate stem cell interactions. Soft Matter. 2010; 6(1):136–143.
55. Huang AH, Yeger-McKeever M, Stein A, Mauck RL. Tensile properties of engineered cartilage formed from chondrocyte- and MSC-laden hydrogels. Osteoarthritis Cartilage. 2008; 16(9):1074–1082. [PubMed: 18353693]

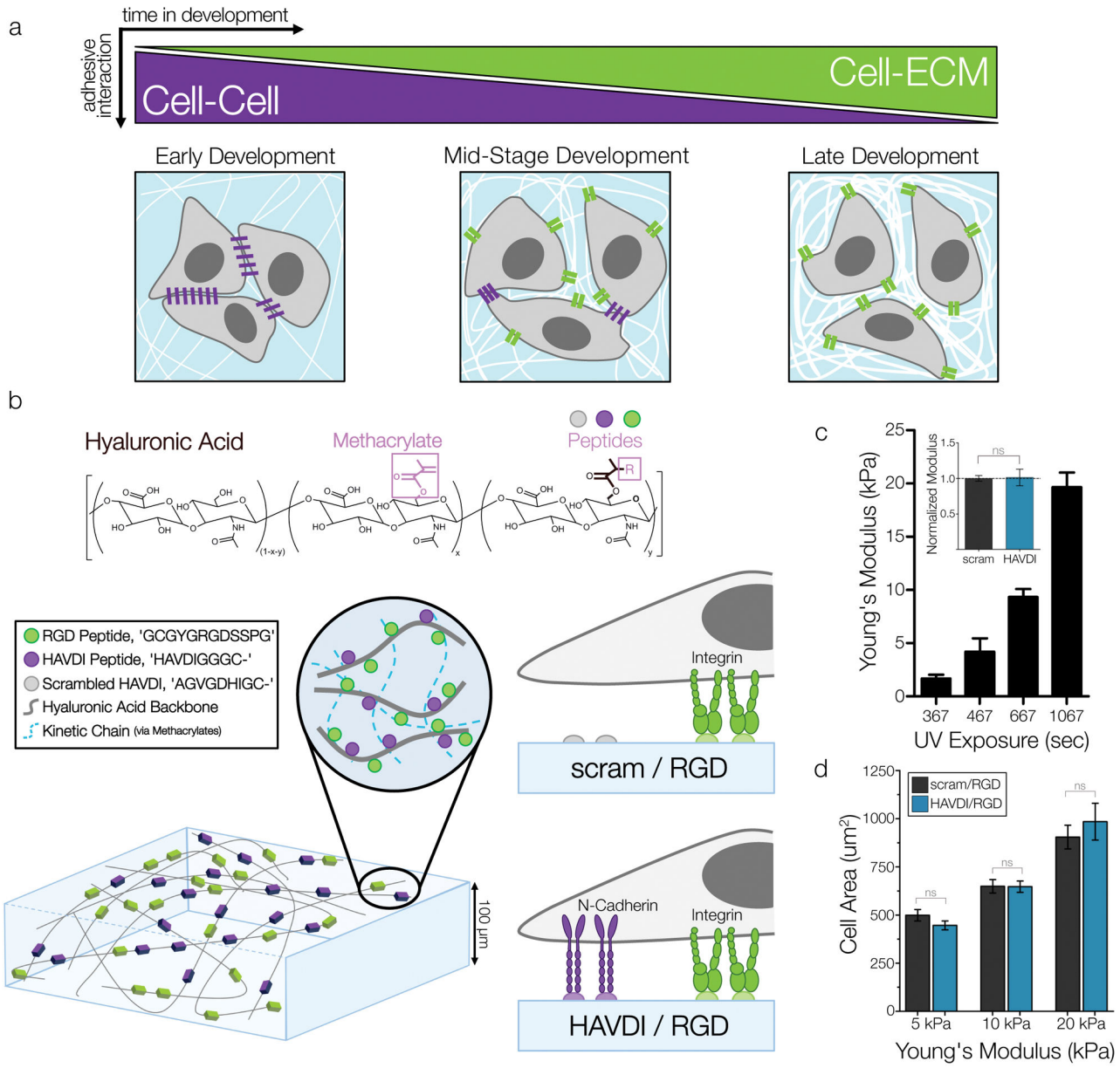

Figure 1. Decoupled presentation of N-Cadherin and Fibronectin adhesive domains to study ECM mechanosensing

(a) Schematic representation of the evolution of the mechanical microenvironment during mesenchymal development. (b) Schematic of methacrylated hyaluronic acid (MeHA) modified with N-Cadherin and Fibronectin adhesive domains and formation into hydrogels via UV-light initiated crosslinking. 'scram/RGD' substrates allow for only integrin-material interactions, while 'HAVDI/RGD' substrates allow for material integrin and cadherin interactions. (c) Control of substrate mechanical properties was achieved by altering UV crosslinking time, as verified by AFM measurements of Young's Modulus (mean ± SD), and normalized comparisons of scram/RGD and HAVDI/RGD moduli across three UV times (*inset*). (d) MSC spread area on increasingly stiff substrates (n>102 cells/group, p>0.6145, mean ± SEM). Scale bars = 10μm.

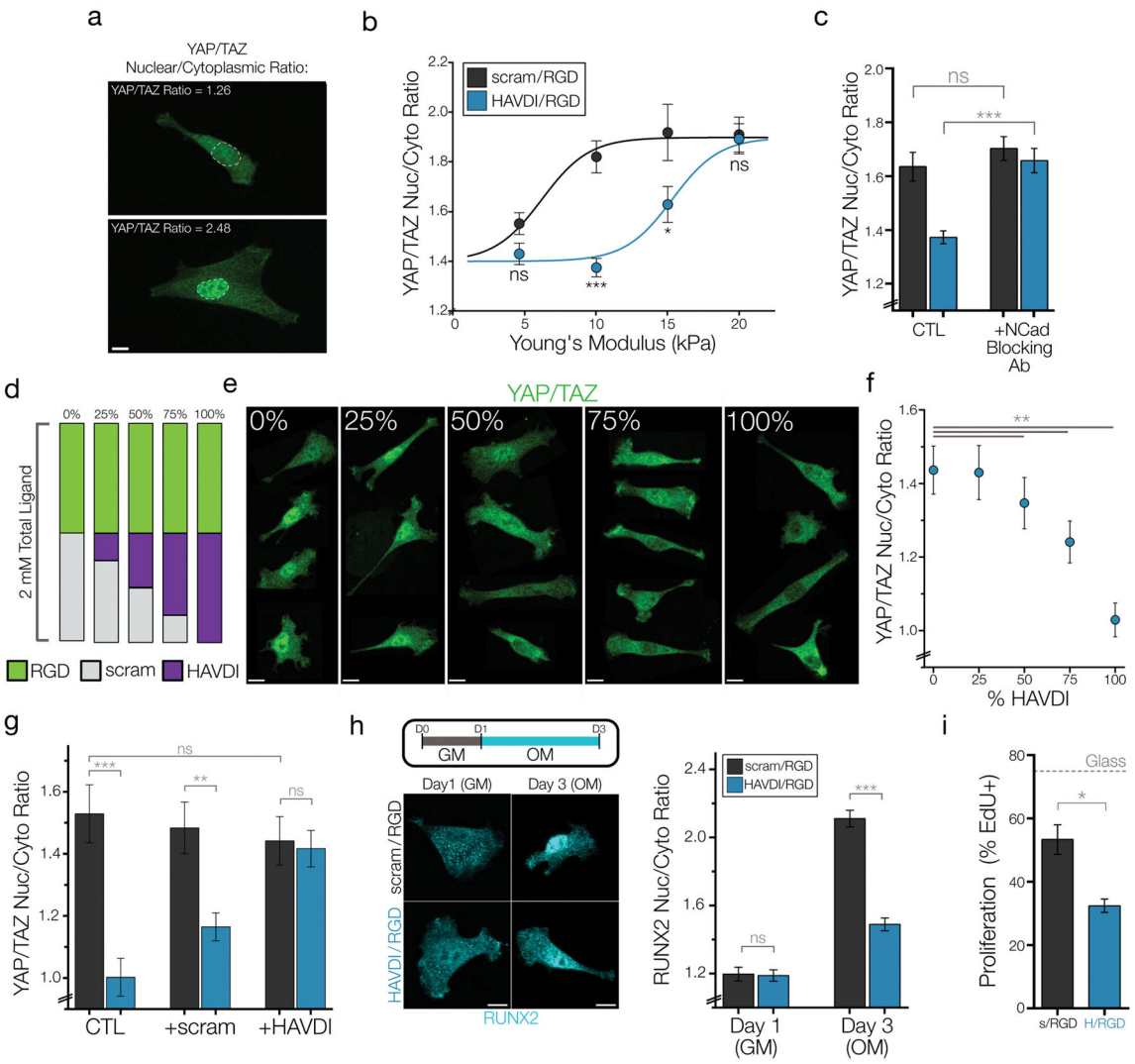

Figure 2. HAVDI ligation reduces the mechanical threshold for YAP/TAZ signaling, altering MSC interpretation of substrate stiffness

(a) Representative quantifications of high and low YAP/TAZ ratios, which were obtained by taking the average intensity in the nucleus and divided by the average intensity of the cytoplasm. (b) YAP/TAZ nuclear to cytoplasmic ratios across a range of substrate stiffness (n>31 cells/group, *=p<0.05, ***=p<0.001 by 2-way ANOVA, mean ± SEM) with corresponding sigmoidal curve-fits. (c) YAP/TAZ ratios after blocking cellular N-Cadherin with a neutralizing antibody prior to seeding on 10 kPa substrates (n>23 cells/group, ***=p<0.001 by 1-Way ANOVA with Bonferroni post-hoc, mean ± SEM). (d) Schematic for assaying dose-dependence of HAVDI presentation on 10 kPa substrates and (e) representative YAP/TAZ images for each group. (f) Quantification of YAP/TAZ ratios with increased presentation of functional HAVDI (n>100 cells/group, **=p<0.01 compared to 0%, by 1-Way ANOVA with Bonferroni post-hoc, mean ± SEM). (g) YAP/TAZ nuclear-to-cytoplasmic ratios following competition with either no peptide (CTL) or 1 mM of soluble peptide in growth media (n>30 cells/group. ***=p<0.001, ** = p<0.01 by 1-Way ANOVA with Bonferroni post-hoc testing, mean ± SEM). (h) (left) Schematic for the early

osteoinduction experiments where GM (growth media) or OM (osteoinductive media) were added over three days and representative images of RUNX2 localization. (right) Quantification of RUNX2 nuclear-to- cytoplasmic ratios. (n>43 cells/group, *** = p<0.001 by 1-Way ANOVA with Bonferroni's post-hoc testing, mean ± SEM). (i) MSC proliferation rate after 48 hrs of culture on 10 kPa substrates, as assayed by the fraction of EdU+ cells (n=3 replicates, measured in 200+ cells per replicate, *=p<0.05, mean ± SEM). Scale bars = 10 μm.

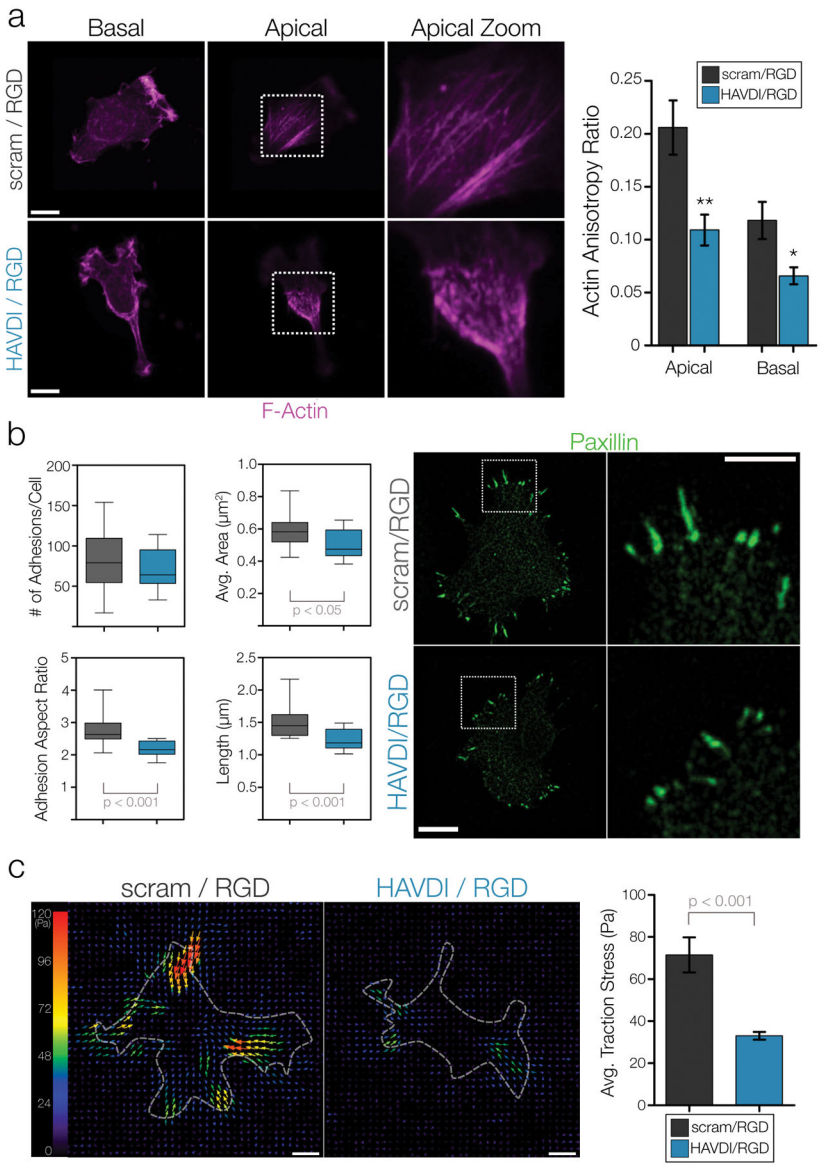

Figure 3. HAVDI/RGD co-presentation attenuates the generation of contractile force

(a) Representative images of F-actin immunofluorescence on the apical and basal planes of MSCs cultured on 10 kPa substrates. Actin organization and polarization was quantified via anisotropy ratios, where more polarized actin yields higher anisotropy ratios (n=14 cells/group, ** = $p<0.01$, * = $p<0.05$ when comparing within planes, mean ± SEM). (b) Paxillin immunostaining for focal adhesions in MSCs on 10 kPa substrates (n=18 cells/group for adhesion number, n>1275 adhesions/group for adhesion area/aspect ratio/length, box plots show 25/50/75th percentile, whiskers show min/max). (c) Representative traction stress vector maps for MSCs plated on 10 kPa substrates. Quantification shows average traction stress generation per cell (n>26 cells/group, mean ± SEM). Scale bars = 10μm.

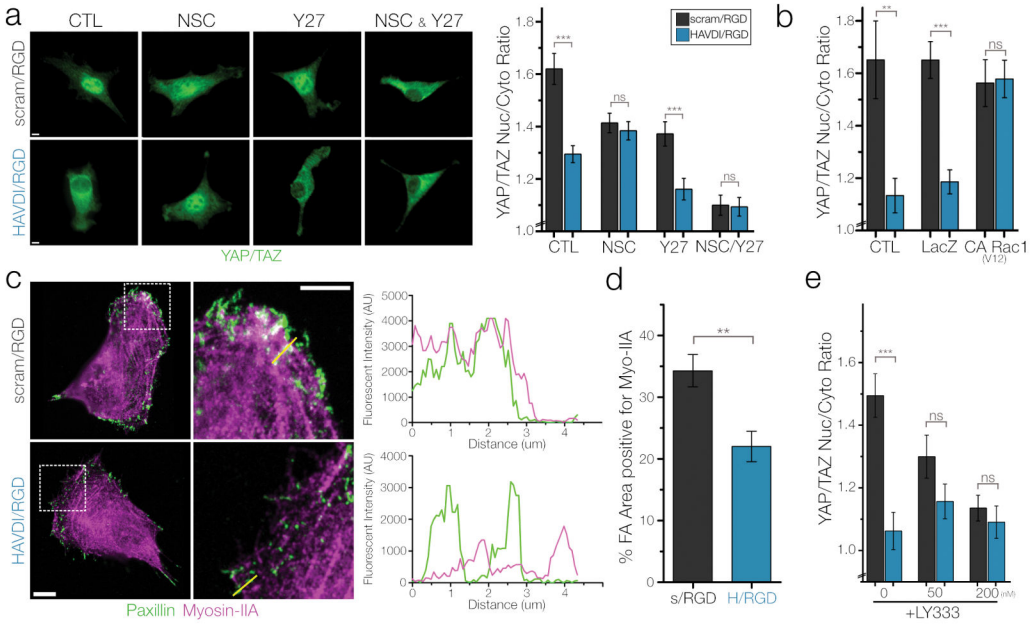

Figure 4. HAVDI ligation alters ECM mechanosensing at intermediate substrate stiffness through Rac1 and Myosin-IIA control of focal adhesion maturation

(a) Representative YAP/TAZ staining and quantification of nuclear to cytoplasmic ratios with pharmacologic inhibition of Rac1 (50 μM NSC-23766) or ROCK (10 μM Y-27632) in MSCs cultured on 10 kPa substrates (n>51 cells/group, ***=p<0.001 by 1-Way ANOVA with Bonferroni post-doc, mean ± SEM). (b) YAP/TAZ ratios after adenoviral transduction of LacZ controls or constitutively active Rac1 on 10 kPa substrates (n>64 cells/group, **=p<0.01, ***=p<0.001 by 1-Way ANOVA with Bonferroni post-hoc, mean ± SEM). (c) Representative confocal images of paxillin and myosin-IIA in MSCs cultured on 10 kPa substrates. Yellow lines in second column indicate pixel regions used to generate intensity profiles. (d) Quantification of focal adhesion area positive for myosin-IIA (n=22 cells/group, **=p<0.01, mean ± SEM). (e) YAP/TAZ ratios following pharmacologic inhibition of PKCβII with 50/200 nM of LY-333531 for 1 hour (n>55 cells/group, ***=p<0.001 by 1-Way ANOVA with Bonferroni post-hoc, mean ± SEM). Scale bars = 10 μm.

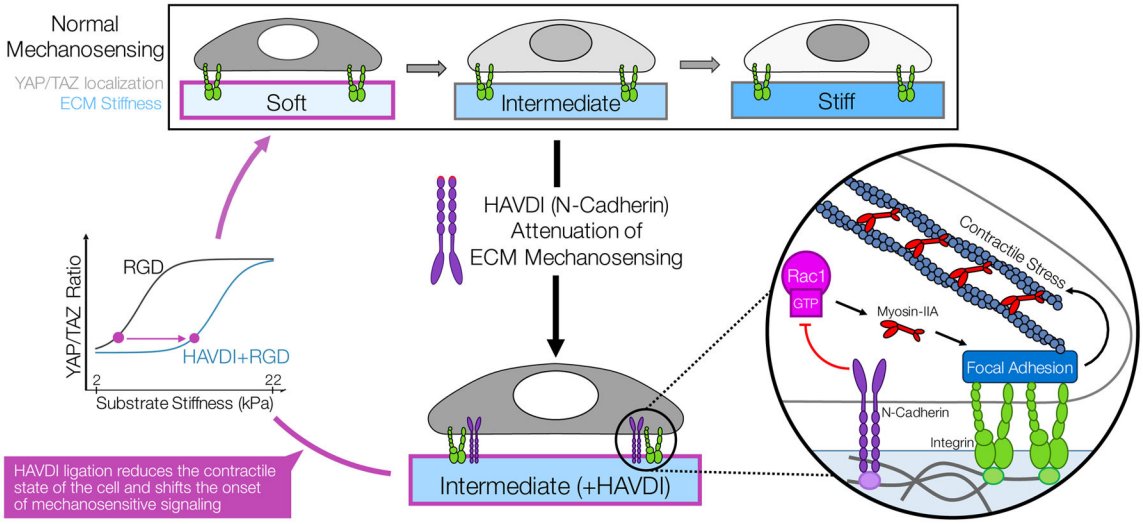

Figure 5. A summary of how HAVDI (from N-Cadherin) ligation can alter MSC mechanosensing of ECM stiffness cues

In normal cell-ECM mechanosensing (in this case, with fibronectin & RGD), as the stiffness of the underlying matrix increases, so does the nuclear-to-cytoplasmic localization of YAP/TAZ. This nuclear YAP/TAZ is a transcriptional regulator of downstream functional outcomes important in progenitor cells. Additional cell-cell contact via N-Cadherin in mesenchymal progenitors acts to attenuate ECM mechanosensing of MSCs by regulating the contractile sate of the cell. In this scenario, N-Cadherin inhibits Rac1-GTP levels, which then results in decreased myosin-IIA incorporation into focal adhesions and reduced contractile force generation. This reduced contractility leads to reduced YAP/TAZ nuclear localization, which thereby influences cell behavior. This attenuation of cell-ECM mechanosensing can lead to progenitor cells behaving as if they were in a different biophysical niche, with cells on intermediate stiffness substrates (~15 kPa) with N-Cadherin and ECM ligation behaving as if they were on a much softer substrate (~6 kPa) with only ECM ligands.